

WHAT CAN WE LEARN FROM COMPARISON BETWEEN CUPRATES AND HE FILMS ? : PHASE SEPARATION AND FLUCTUATING SUPERFLUIDITY

Y. J. UEMURA

Dept. of Physics, Columbia University, New York, NY 10027, U. S. A.

E-mail: tomo@kirby.phys.columbia.edu

In the underdoped, overdoped, Zn-doped or stripe-forming regions of high- T_c cuprate superconductors (HTSC), the superfluid density n_s/m^* at $T \rightarrow 0$ shows universal correlations with T_c . Similar strong correlations exist between 2-dimensional superfluid density and superfluid transition temperature in thin films of ^4He in non-porous or porous media, and $^4\text{He}/^3\text{He}$ film adsorbed on porous media. Based on analogy between HTSC and He film systems, we propose a model for cuprates where: (1) the overdoped region is characterized by a phase separation similar to $^4\text{He}/^3\text{He}$; and (2) pair (boson) formation and fluctuating superconductivity occur at separate temperatures above T_c in the underdoped region.

The magnetic field penetration depth λ of superconductors is related to the superconducting carrier density n_s divided by the effective mass m^* , as $1/\lambda^2 \propto n_s/m^*$. In this paper, we shall refer to n_s/m^* as the “superfluid density”. Since the discovery of HTSC, we have performed muon spin relaxation (μSR) studies of under- to optimally doped [1,2], overdoped [3], and Zn-doped [4] cuprates, as well as HTSC systems associated with the formation of static spin stripes [5,6]. In all of these systems, we found strong correlations between n_s/m^* at $T \rightarrow 0$ and T_c , as shown in Fig. 1. This figure suggests that the superfluid density is likely a crucial determining factor for T_c of all these HTSC systems. These correlations in the underdoped region have been interpreted in terms of Bose-Einstein (BE) to BCS crossover [7-9], phase fluctuations [10], XY-model [11], as well as via RVB-type [12] pictures.

Thin films of ^4He also exhibit strong correlations between their two-dimensional superfluid area density n_{s2d}/m^* and T_c . In Figure 2, we replot published results of ^4He film on mylar sheet (non-porous media) [13], vycor glass (porous media) [14,15], as well as thin film $^4\text{He}/^3\text{He}$ mixture on alumina powder (porous media) [16]. The horizontal axis was obtained after converting the He coverage into 2-dimensional (2-d) areal boson density divided by the boson mass n_{b2d}/m_b , and then into the 2-d Fermi temperature T_{F2d} assuming $n_{b2d} = n_{s2d}/2$ and $m_b = 2m^*$. The Kosterlitz-Thouless (KT) transition temperature $T_{KT} = T_{F2d}/8$ for the strong coupling limit [17] is shown by the solid line. T_c scales with T_{KT} , as expected for an ideal Bose gas composed of tightly-bound fermion pairs in a pure 2-d environment.

Figures 1 and 2 exhibit striking resemblance. In Zn-doped HTSC systems [4], the superfluid density n_s/m^* at $T \rightarrow 0$ decreases with increasing Zn concentration as shown in Fig. 3(a). To explain this result, we proposed a “swiss cheese model” [4], where each Zn suppresses superconductivity of the surrounding region characterized by the in-plane coherence ξ_{ab} on the CuO_2 planes, as illustrated in Fig. 3(d). The solid lines represent the expected superfluid density estimated from the ratio of superconducting versus non-superconducting regions. Without any fitting, this

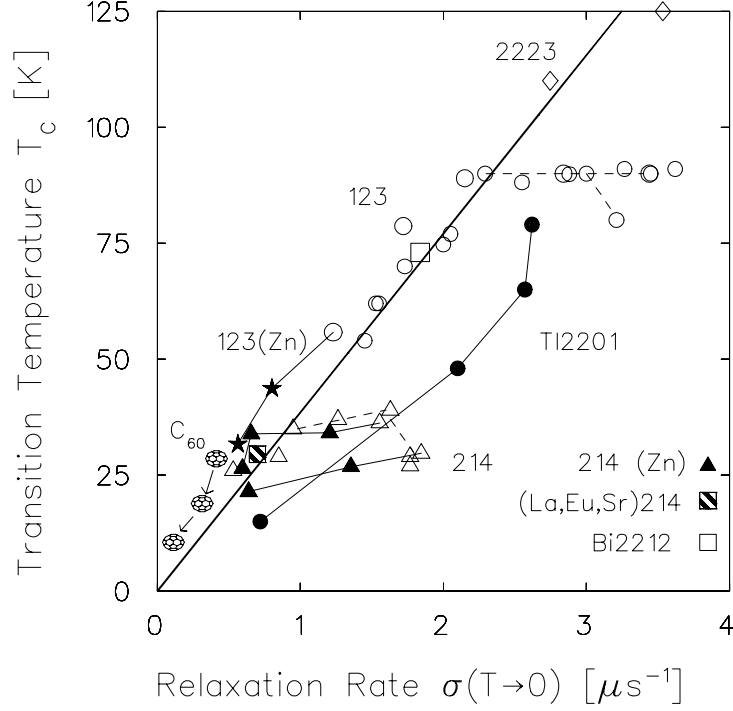


Figure 1. Superconducting transition temperature T_c of HTSC systems plotted versus muon spin relaxation rate $\sigma(T \rightarrow 0) \propto 1/\lambda^2 \propto n_s/m^*$ [1-5]. Y123 systems on the solid line are in the underdoped region, while Tl2201 systems are in the overdoped region.

model gives a very good agreement with the experimental data. Recently this picture was confirmed directly by the scanning tunnelling microscope studies of Pan et al. [18].

As shown in Fig. 1, T_c of the Zn-doped cuprates follow the trajectory of hole-doped cuprates without Zn [4]. This suggests that Zn reduces n_s/m^* , and the volume average value of n_s/m^* then determines T_c . This situation looks quite analogous to ^4He films adsorbed on porous media, where a part of He forms a normal layer (i.e. a “healing layer”) between the porous substrate and superfluid, while T_c is determined by the amount of the superfluid portion.

Recently, Kojima *et al.* [5] found that $\text{La}_{1.75}\text{Eu}_{0.1}\text{Sr}_{0.15}\text{CuO}_4$ (LESCO) undergoes magnetic order with static stripe freezing occurring in about half of the volume fraction below $T_N \sim 10$ K. This system becomes superconducting below $T_c \sim 30$ K. The superfluid density could be determined even below T_N , thanks to the signal from the remaining non-magnetic volume. The results show that n_s/m^* is reduced to about a half of the value for $\text{La}_{1.85}\text{Sr}_{0.15}\text{CuO}_4$ without stripe formation. This is consistent with a picture where hole carriers in the regions with the frozen static spin stripes do not participate in the superfluid. As shown in Fig. 1, T_c again scales with the volume averaged value of n_s/m^* in LESCO with static stripes. Similar scaling with the trends of other 214 cuprates has been found in the μSR results of

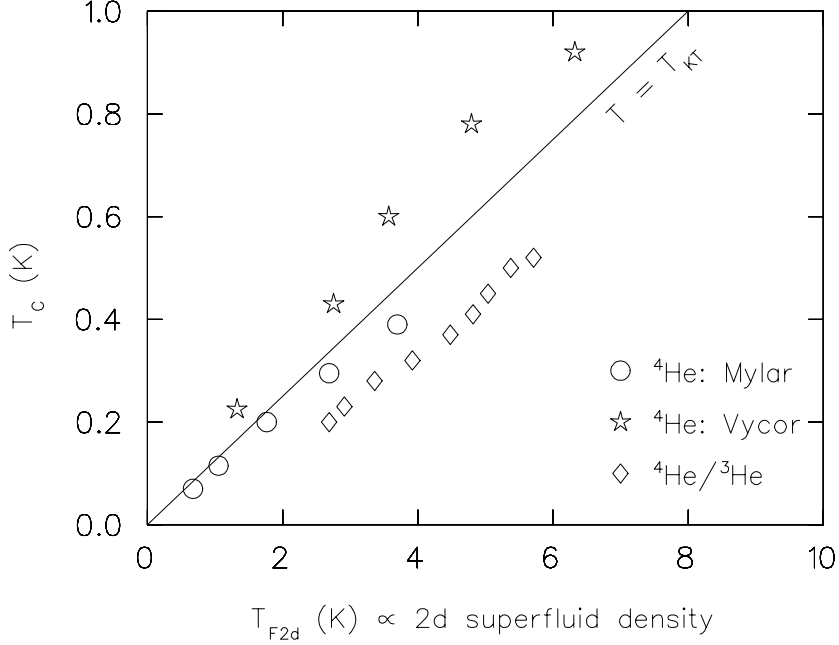


Figure 2. Superfluid transition temperature T_c of ^4He film adsorbed on Mylar film [13], porous Vicor glass [14,15] and $^4\text{He}/^3\text{He}$ mixture adsorbed on fine alumina powder [16], plotted versus 2-d superfluid density at $T \rightarrow 0$. The horizontal axis is shown by converting 2-d boson density n_{b2d} and mass m_b into fermionic language as $n_{b2d} = n_{s2d}/2$ and $m_b = 2m^*$ and then calculating the corresponding 2-d Fermi temperature $T_{F2d} \propto n_{s2d}/m^*$. The solid line indicates the superfluid density expected at the Kosterlitz-Thouless transition temperature T_{KT} .

T_c versus n_s/m^* in single crystals of $\text{La}_2\text{CuO}_{4.12}$ and $\text{La}_{1.88}\text{Sr}_{0.12}\text{CuO}_4$ [6], both of which having stripe spin freezing detected in a partial volume fraction of muon sites. The region with frozen stripes, though its size and origin are yet to be clarified, looks analogous to the non-superconducting region around Zn in Zn-doped cuprates.

In overdoped Tl2201, μSR studies [3,19] revealed that n_s/m^* decreases with increasing hole doping, as shown in Fig. 3(b). Since no signature of anomalous behavior has been found for m^* , this result suggests that n_s becomes smaller than the normal state carrier concentration n_n . Indeed a specific heat study in Tl2201 [20] suggests co-existence of gapped (A) and un-gapped (B) responses, with the latter portion increasing with increasing doping. These results can be explained if we assume a microscopic phase separation between superfluid and non-superconducting fermionic carriers [3,8,9,21], as illustrated in Fig. 3(d).

A mixture of ^4He and ^3He provides a typical example of phase separation. With an increasing fermionic portion of ^3He , T_c decreases, maintaining an approximate proportionality to $p_4^{2/3}$ where p_4 denotes the volume fraction of ^4He . Thin films of $^4\text{He}/^3\text{He}$ can be adsorbed on porous media, such as fine alumina powders, which constrain the phase separation to be microscopic. In Fig. 3(c), we show the re-

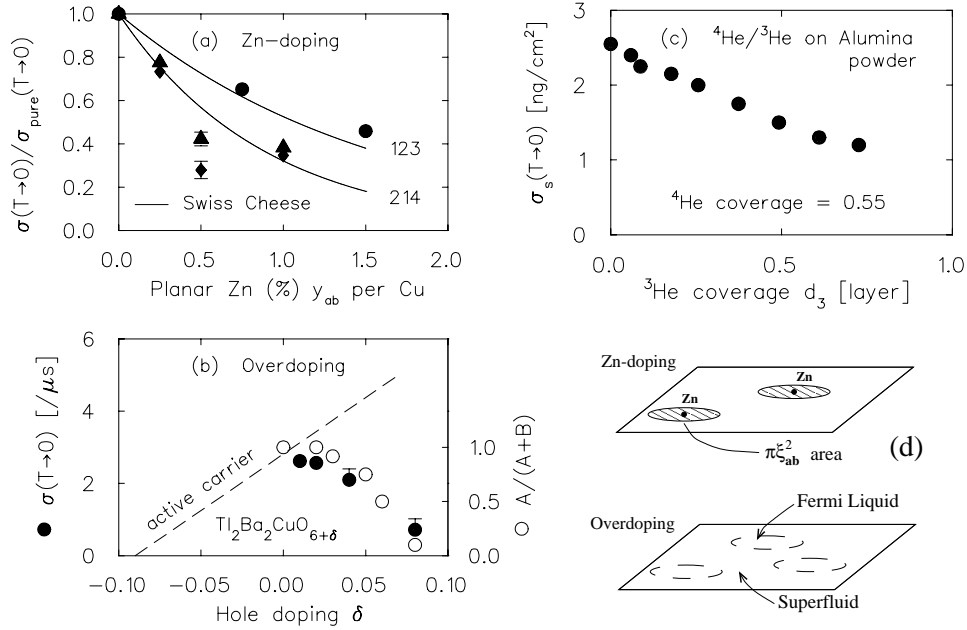


Figure 3. Depletion of the superfluid density due to perturbation: (a) Zn-doping in YBa₂Cu₃O_{6.63}, La_{1.85}Sr_{0.15}CuO₄ and La_{1.8}Sr_{0.2}CuO₄ [4]; (b) Overdoping in Tl₂Ba₂CuO_{6+δ} [3]; and (c) ³He mixing in ⁴He film adsorbed on fine alumina powder [16]. (d) illustrates the Swiss cheese model with Zn doping [4], and proposed phase separation in overdoped HTSC. Open circles in (b) represents the relative weight of the gapped response (A) normalized to the sum of gapped (A) and ungapped (B) responses in the linear-*T* term of the specific heat measurements by Loram *et al.* [20].

duction of superfluid density with increasing ³He fraction p_3 using the results in ref. [16]. In this case, due to the 2-d configuration, T_c decreases approximately as $T_c \propto p_4 = (1 - p_3)$. Thus, both in ⁴He/³He and in overdoped Tl2201, we see a suppression of the superfluid density and T_c due to increasing fermionic fraction in a microscopic phase separation.

Based on these analogies, we propose a new phase diagram for HTSC systems in Fig. 4. As stated in our previous publications [7-9,21], we consider the “pseudo-gap” temperature T^* to represent a signature of pair (boson) formation. In this case, T^* reflects the magnitude of the attractive interaction between fermionic carriers. If this attractive interaction rapidly decreases with increasing hole doping near the “optimal T_c ” region, there is no robust superconductivity in the overdoped region. However, the system can phase separate into regions with “optimal hole density (OHD)” (corresponding to “optimal T_c ”) which maintain superconductivity and those with higher hole density (HHD) without superconductivity. The charge imbalance will cost extra energy to phase separate while bulk superconductivity could gain condensation energy. The OHD region would correspond to the ⁴He-rich superfluid while HHD region to the ³He-rich normal fluid in analogy to ⁴He/³He.

Recently Loram, Tallon and co-workers [22] noticed a sharp reduction of the T^*

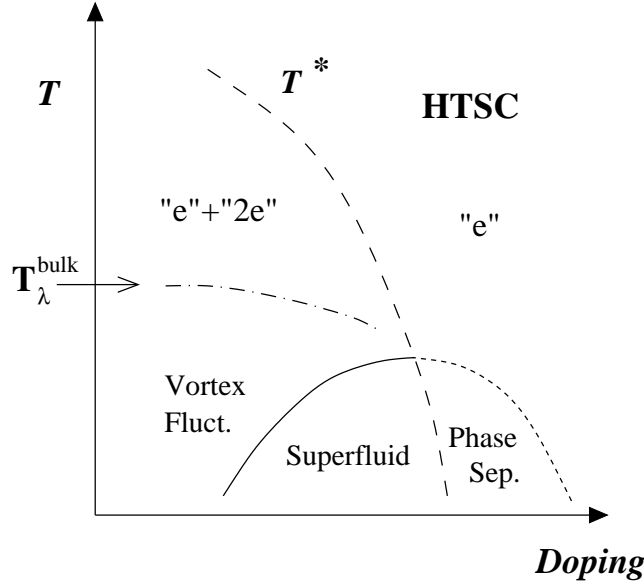


Figure 4. Proposed new phase diagram for HTSC systems. With decreasing temperature in the underdoped side, individual fermion carriers starts forming pairs below T^* , and time-dependent superconductivity appears below T_λ . In the overdoped side, there is no pairing interaction, and superconductivity survives via phase separation.

line near the hole concentration of $x \sim 0.19$ per Cu. They argued that this phenomenon is incompatible with superconductivity observed at $x \geq 0.19$ in the overdoped region, if T^* represents the superconducting pairing interaction. However, our picture with phase separation provides a way to reconcile the sharp reduction of the pairing energy scale T^* with the survival of superconductivity in the overdoped region.

Signatures of fluctuating superconductivity have been found in the underdoped cuprates above T_c in studies of high-frequency optical conductivity σ_{ac} [23], the Nernst effect [24], and the “resonance” inelastic scattering intensity in neutron scattering [25]. We notice that all these results show onset of their effect below $T \sim 150$ K, which is substantially lower than T^* determined from the c-axis conductivity [26] and/or NMR Knight shift [27]. The analogy to He films can provide a possible explanation to this feature.

In the case of He, formation of bosons (He atoms) from fermions occurs at very high temperatures. At a much lower temperature $T_\lambda^{bulk} = 2.2$ K (the bulk λ transition point) BE condensation occurs in a 3-d environment. In a highly 2-d environment, the bulk superfluidity occurs at lower temperature T_c . Time-dependent superfluidity via un-bound vortices occurs between T_c and T_λ in the 2-d situation. Similarly to this, we expect the two step process, i.e., pair formation at a high temperature T^* followed by signatures of fluctuating superconductivity at much lower temperature below T_λ ($T_c < T_\lambda < T^*$) for underdoped cuprates, as

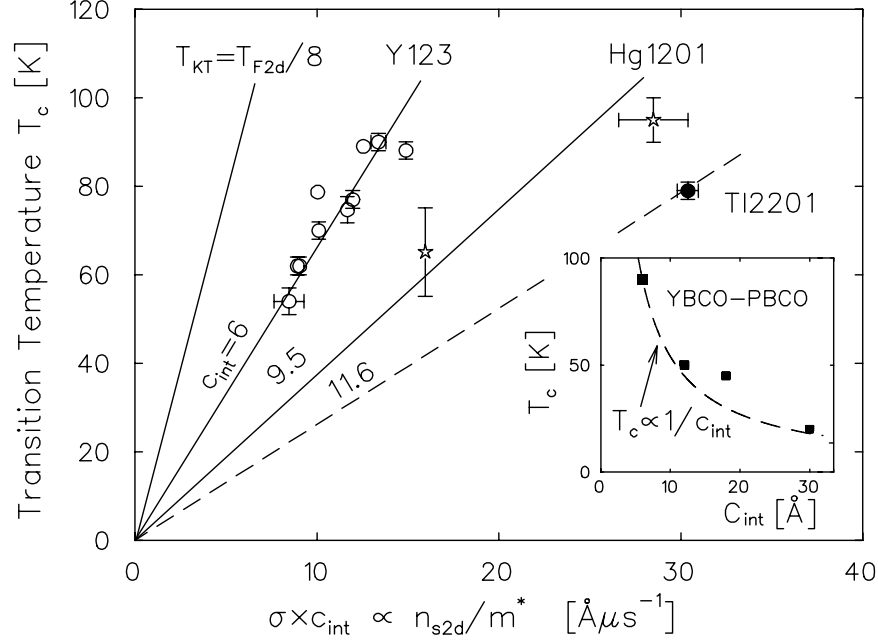


Figure 5. Plot of T_c versus $\sigma \times c_{int} \propto n_{s2d}/m^* \propto T_{F2d}$ in underdoped and nearly optimally-doped HTSC [1,3,28] systems. T_{KT} shows the strong coupling limit in pure 2-d. Inset: T_c vs. c_{int} in multilayer YBCO-PrBCO films [29].

illustrated in Fig. 4. We can ascribe the σ_{ac} , Nernst, and neutron results to the onset of time-dependent superconductivity below T_λ while the c-axis transport and Knight shift to the formation of singlet fermion pairs below T^* . Formation of a pair (boson) does not immediately correspond to quantum condensation, which requires a certain density/mass to achieve phase coherence of bosonic wave functions.

Despite all these analogous features, there exists an important difference between HTSC and He films. Figure 5 shows a plot of T_c versus the 2-d area superfluid density n_{s2d}/m^* obtained for cuprates by multiplying n_s/m^* with the average distance c_{int} between the CuO_2 planes. We notice that: (A) T_c for the cuprates are 2-4 times reduced from T_{KT} calculated for the strong-coupling limit; (B) for a given n_{s2d}/m^* , T_c is higher for systems with smaller c_{int} (consistent with the results in inset for YBCO-PBCO multilayer films). The feature (B) is incompatible with the KT transition in pure 2-d systems where T_c should not depend on a 3-d coupling via c_{int} . Previously, we pointed out that BE condensation in quasi 2-d systems would provide a better account for the observed dependence of T_c on c_{int} [9,21].

Finally, we would like to point out that fluctuating superconductivity can be expected not only for the KT transition but also for BE-condensation in quasi 2-d systems. Analogous, for example, to spin fluctuations in quasi 2-d magnetic systems, correlations develop already at the temperature corresponding the transition temperature T_{c3d} for a 3-d environment, while long-range order occurs at a much

lower temperature T_{c2d} due to dimensionality effects. The correlated spin fluctuations at $T_{c2d} < T < T_{c3d}$ correspond to the fluctuating superfluidity in HTSC and ^4He . In BE condensation in the quasi 2-d situation, T_c is determined at a point where thermal energy becomes comparable to the interlayer interaction enhanced by the fluctuating in-plane superconducting correlations. This process is essentially similar to how T_c for magnetic order is determined in quasi 2-d spin systems. Thus, the σ_{ac} , Nernst, and neutron results cannot distinguish between a pure KT transition versus quasi 2-d BE condensation. This point requires further studies.

Acknowledgement

The author is grateful to M. Randeria for helpful discussions. This study is supported by NSF (DMR-98-02000) and US-Israeli Binational Science Foundation.

References

1. Y.J. Uemura *et al.*, Phys. Rev. Lett. **62** (1989) 2317-2320.
2. Y.J. Uemura *et al.*, Phys. Rev. Lett. **66** (1991) 2665-2668.
3. Y.J. Uemura *et al.*, Nature **364** (1993) 605-607.
4. B. Nachumi *et al.*, Phys. Rev. Lett. **77** (1996) 5421-5424.
5. K.M. Kojima *et al.*, submitted to Phys. Rev. Lett. (2000).
6. A. Savici *et al.*, Physica **B289-290** (2000) 338-342.; and unpublished
7. Y.J. Uemura, in *Proceedings of the Workshop in Polarons and Bipolarons in High- T_c Superconductors and Related Materials, Cambridge, 1994* ed. by E. Salje *et al.* (Cambridge Univ. Press, 1995) p.p. 453-460;
8. Y.J. Uemura, in *Proceedings of the CCAST Symposium on High- T_c Superconductivity and the C_{60} Family, Beijing, 1994* ed. by S. Feng and H.C. Ren (Gordon and Breach, New York, 1995) pp. 113-142.
9. Y.J. Uemura, Physica **C282-287** (1997) 194-197.
10. V.J. Emery and S. Kivelson, Nature **374** (1995) 434-437.
11. T. Schneider, Z. Phys. **B88** (1992) 249-253; T. Schneider and H. Keller, Int. J. Mod. Phys. **8** (1993) 487-528.
12. P.A. Lee and N. Nagaosa, Phys. Rev. **B46** (1992) 5621-5639; P.A. Lee and X.G. Wen, Phys. Rev. Lett. **78** (1997) 4111-4115.
13. G. Agnolet, D.F. McQueeney and J.D. Reppy, Phys. Rev. **B39** (1989) 8934-8958.
14. D.J. Bishop, J.E. Berthold, J.M. Parpia and J.D. Reppy, Phys. Rev. **B24** (1981) 5047-5057.
15. K. Shirahama, M. Kubota, S. Ogawa, N. Wada, T. Watanabe, Phys. Rev. Lett. **64** (1990) 1541-1544; P.A. Crowell, F.W. Van Keuls, and J.D. Reppy, Phys. Rev. **B55** (1997) 12620-12634.
16. H. Chyo and G.A. Williams, J. Low Temp. Phys. **110** (1998) 533-538.
17. E. Babaev and H. Kleinert, Phys. Rev. **B59** (1999) 12083-12089.
18. S.H. Pan *et al.*, Nature **403** (2000) 746-750.
19. Ch. Niedermayer *et al.*, Phys. Rev. Lett. **71** (1993) 1764-1767.

20. J.W. Loram, K.A. Mirza, J.M. Wade, J.R. Cooper, and W.Y. Liang, *Physica* **C235-240** (1994) 134-137.
21. Y.J. Uemura, invited paper presented at the M2S-HTSC-VI Conference in Houston, Feb., 2000, *Physica C* in press.
22. J.W. Loram, J. Lou, J.R. Cooper, W.Y. Liang and J.L. Tallon, presented at Crest International Workshop, Nagoya, Japan, January, 2000, *J. Phys. Chem. Solids*. in press; and references therein.
23. J. Corson, R. Mallozzi, J. Orenstein, J.N. Eckstein, I. Bozovic, *Nature* **398** (1999) 221-223.
24. Z.A. Xu, N.P. Ong, Y. Wang, T. Kakeshita and S. Uchida, *Nature* **406** (2000) 486-489.
25. P. Dai, H.A. Mook, G. Aeppli, S.M. Hayden, F. Dogan, *Nature* **406** (2000) 965-968.
26. T. Ito, T. Ido, H. Takagi and S. Uchida, *Nature* **350** (1991) 569-572.
27. See, for example, H. Alloul, T. Ohno, P. Mendels, *Phys. Rev. Lett.* **63** (1989) 1700-1703.
28. B. Nachumi *et al.*, *Hyperfine Interact.* **105** (1997) 119-124.
29. O. Fischer *et al.*, *Physica* **B169** (1991) 116.